---

**Article:**
Douterelo, I., Fish, K.E. orcid.org/0000-0002-3265-2826 and Boxall, J.B. orcid.org/0000-0002-4681-6895 (2018) Succession of bacterial and fungal communities within biofilms of a chlorinated drinking water distribution system. Water Research, 141. pp. 74-85. ISSN 0043-1354

https://doi.org/10.1016/j.watres.2018.04.058

---

Water Research 141 (2018) 74–85

Contents lists available at ScienceDirect

Water Research

journal homepage: www.elsevier.com/locate/watres

# Succession of bacterial and fungal communities within biofilms of a chlorinated drinking water distribution system

I. Douterelo*, K.E. Fish, J.B. Boxall

*Pennine Water Group, Department of Civil and Structural Engineering, Mappin Street, University of Sheffield, Sheffield, S1 3JD, UK*

ARTICLE INFO

*Article history:*
Received 14 December 2017
Received in revised form
5 April 2018
Accepted 25 April 2018
Available online 3 May 2018

*Keywords:*
Fungal-bacterial interactions
Biofilm
Drinking water
Selection
Succession

ABSTRACT

Understanding the temporal dynamics of multi-species biofilms in Drinking Water Distribution Systems (DWDS) is essential to ensure safe, high quality water reaches consumers after it passes through these high surface area reactors. This research studied the succession characteristics of fungal and bacterial communities under controlled environmental conditions fully representative of operational DWDS.

Microbial communities were observed to increase in complexity after one month of biofilm development but they did not reach stability after three months. Changes in cell numbers were faster at the start of biofilm formation and tended to decrease over time, despite the continuing changes in bacterial community composition. Fungal diversity was markedly less than bacterial diversity and had a lag in responding to temporal dynamics. A core-mixed community of bacteria including *Pseudomonas*, *Massillia* and *Sphingomonas* and the fungi *Acremonium* and *Neocosmopora* were present constantly and consistently in the biofilms over time and conditions studied.

Monitoring and managing biofilms and such ubiquitous core microbial communities are key control strategies to ensuring the delivery of safe drinking water via the current ageing DWDS infrastructure.



## 1. Introduction

The delivery of high-quality, safe drinking water depends, to a large extent, on the optimal operation of the transportation infrastructure known as Drinking Water Distribution Systems (DWDS). DWDS are complex pipe networks which function as dynamic ecosystems where microorganisms, dominated by those attached within biofilms on the inner pipe surfaces, are involved in a range of processes that ultimately determine the quality of the delivered water. Microbial dynamics in any ecosystem are determined by interactions between microorganisms and environmental factors. However, within DWDS these microbial dynamics and their temporal variation regarding inter-taxa biofilms remain largely unexplored.

Most DWDS management strategies consider only planktonic microorganisms, free organisms transported in the bulk water. Reinforced by legislation that only obliges water utilities to analyse bulk water samples from service reservoirs and customer taps and using plate counting techniques and faecal indicators as a measurement of failures in the system. However, the majority of the microbial biomass in DWDS is found attached to the inner surfaces of pipes forming microbial consortiums known as biofilms, rather than in the water column (Flemming, 1998). Biofilms provide advantages to embedded microorganisms, including sharing of nutrients and metabolic products and facilitation of resistance to environmental stress (Chao et al., 2015). Microorganisms within biofilms can be associated with several processes occurring in DWDS. Biofilms can affect directly the infrastructure via biocorrosion of metal pipes (Wang et al., 2012) and/or modify general water characteristics (Lehtola et al., 2004) and trigger discolouration events through the mobilisation of the attached biofilm into the bulk water (Husband et al., 2016). Another major concern is the potential for biofilms to act as reservoirs of opportunistic pathogens (Wingender and Flemming, 2011; Douterelo et al., 2014a). The most widespread strategies used to control microorganisms in the bulk water of DWDS is the quality of the water as it leaves the treatment works and/or the use of a disinfectant residual in the bulk water, mainly chlorine or chloramine. The efficiency of these strategies to control biofilm formation and properties is limited (Schwering et al., 2013). There are no standard methods to monitor or control the growth of biofilms in DWDS and, despite their importance, biofilms are normally neglected when management

* Corresponding author.
*E-mail address:* i.douterelo@sheffield.ac.uk (I. Douterelo).

https://doi.org/10.1016/j.watres.2018.04.058

and control strategies are designed.

Biofilm formation is a successional process (Martiny et al., 2003; Prest et al., 2016) beginning when free-living microorganisms colonize and attach to pipe surfaces, growing whilst generating extracellular polymeric substances (EPS) and modifying the pipe environment in a way that supports or excludes the incorporation of other microorganisms into the biofilm. However, most of the studies reporting data on the microbiology of DWDS occur over relatively short time frames (Simoes et al., 2010; Douterelo et al., 2013) and evaluate mainly the temporal-spatial dynamics in bulk water samples (Hoefel et al., 2005; van der Wielen and van der Kooij, 2010; Roeselers et al., 2015) or biofilm growth in reactors (Gomes et al., 2014; Revetta et al., 2016). Improving our understanding of biofilm behaviour in these systems requires long-term series data of the attached microbial phase.

Commonly overlooked in DWDS studies is the fact that biofilms are formed by a complex amalgamate of microorganisms. Microbiologists working in DWDS often focus on one taxonomic group, predominately bacteria (Revetta et al., 2010; Liu et al., 2014a; Vaz-Moreira et al., 2017) or a specific group of bacteria (Gomez-Alvarez et al., 2016) despite evidence that other microbial taxa such as fungi, viruses and amoeba are present in biofilms (Wingender and Flemming, 2011; Buse et al., 2013; Ashbolt, 2015; Fish et al., 2015; Douterelo et al., 2016a). Knowledge on the interactions between different microbial strains in actual biofilms is still at its infancy, understanding how the full microbial consortium forms, how different microbial strains interact, when these interactions start and who the main drivers of change are remains largely unknown. Advances in microscopy and molecular methods are now available that allow a better understanding of microbial communities dynamics including new sequencing platforms.

The aim of the research reported here was to study the dynamics and temporal patterns of fully representative DWDS biofilm community development and succession over a three-month period. We particularly aimed to study correlations between bacteria and fungi and biofilm cellular developmental rates that have been traditionally overlooked in drinking water studies. Such bacterial-fungal community characteristics and their impact upon biofilm development/formation needs to be understood in order to find patterns of microbial behaviour that can inform modelling, and management strategies such as disinfectant residual.

## 2. Methods

In order to meet the specific aims, a holistic approach was adopted combining environmental physico-chemical analysis, microscopy and molecular methods to study the process of biofilm formation and maturation. These were applied to samples obtained from the pipe wall of a full scale, temperature controlled experimental pipe facility that fully replicates the conditions of an operational DWDS. This study comprises a range of methods that allow characterization at physiological (cell volume and spread) and phylogenetic levels (gene quantification and taxonomic characterization) yielding a more comprehensive understanding of microbial dynamics over time.

### 2.1. Experimental facility

The experiment was carried out using a DWDS test facility which comprised a pipe loop fed with water from the local water supply via an independent tank and pump (Fig. 1), which recirculated water around the pipe loop. An independent system residence time of 24 h was set using a trickle-feed and drain to provide representative water quality. The pipe loop consists of 9.5 × 21.4 m long coils of 79.3 mm internal diameter High-Density Polyethylene (HDPE) pipe, thus has a total length of 203 m such that pipe surface area is dominant over ancillaries (Fig. 1B). HDPE was selected as it is a prevalent and representative material used in DWDS world-wide (WHO, 2006). The room temperature of the experimental facility was set to 16 °C for all results reported here; this is representative of average spring and summer water temperatures in UK DWDS.

Before experiments commenced, the pipe loop was set to an initial state by disinfection with 20 mg/l of RODOLITE H (RODOL Ltd, Liverpool, UK); a solution of sodium hypochlorite with less than 16% free chlorine. Then the system was run at maximum flow rate (4.2 l/s) for 24 h and flushed afterwards at the maximum flow rate with fresh water until the levels of chlorine were similar to those of the local tap water. After disinfecting the system, sterile PWG coupons (Deines et al., 2010) were fitted along and around the sample length of the pipe loop. The PWG coupons have an insert suitable for direct microscopy observations and an outer part that allows for obtaining biofilm biomass for subsequent molecular analysis (Fig. 1A).

For the experiments reported here a varied flow hydraulic profile was applied based on daily patterns observed in real DWDS in the UK. The regime follows a typical domestic dominated diurnal pattern with night time low flow of 0.2 l/s and morning peak flow of 0.5 l/s. This is the low varied flow regime originally reported and used in (Husband et al., 2008). The daily regime was repeated for a growth phase of 84 days.

### 2.2. Physico-chemical analysis of water quality

Triplicate bulk water samples were collected on days 0, 14, 34, 42, 52, 70 and 84 during the growth phase. Free chlorine was measured on site at the time of sampling using a HACH DR/2010 spectrophotometer. Measurements of temperature and pH were also made on site at the time of sampling using a Hanna H1991003 m. Water samples for Total Organic Carbon (TOC), iron and manganese were sent to an independent accredited laboratory; AlControl Laboratories (Rotherham, UK) for analysis. Turbidity was constantly measured by an ATI A15/76 turbidity monitor (ATI, Delph, UK) installed in the experimental facility.

### 2.3. Confocal laser scanning microscopy (CLSM)

CLSM was used to obtain images of biofilm and enable the quantification of the cell coverage on the coupon surfaces. Three coupons were studied for each sampling day from day 0 (used as a control) to days 14, 34, 42, 52, 70 and 84. For this analysis the insert of the PWG coupon was removed and fixed in 5% formaldehyde for 24 h and then transferred to phosphate buffer solution (PBS) and stored at 4 °C until analysed. After fixing, the inserts were stained with 20 μmol $l^{-1}$ Syto® 63, a cell-permeative nucleic acid stain, (Molecular Probes, Invitrogen, UK) for 30 min at room temperature. Imaging was performed using a Zeiss LSM 510 Meta Confocal Florescent Microscope at the Kroto Imaging Facility at The University of Sheffield and the LSM 510 Image Examiner Software (Zeiss, UK). Each insert was imaged for seven random fields of view (FOV) to generate lambda z-stacks from which the cell stain signal was isolated and quantified, as described in detail in Fish et al. (2015). The images were then processed to obtain a relative quantification of the cell coverage (i.e. volume of cells and their spread) at each layer (Fish et al., 2015). The resultant dataset was analysed using Python and R to calculate the volume and spread of the cells (see Fish et al., 2015 for detailed methods). For each sample day replication was n = 21, apart from Day 0 (n = 20) and Day 82 (n = 19) where FOV were corrupted or removed as an outlier.

Differences among days in biofilm cell volume and spread were tested statistically using non-parametric tests; the Kruskall-Wallis

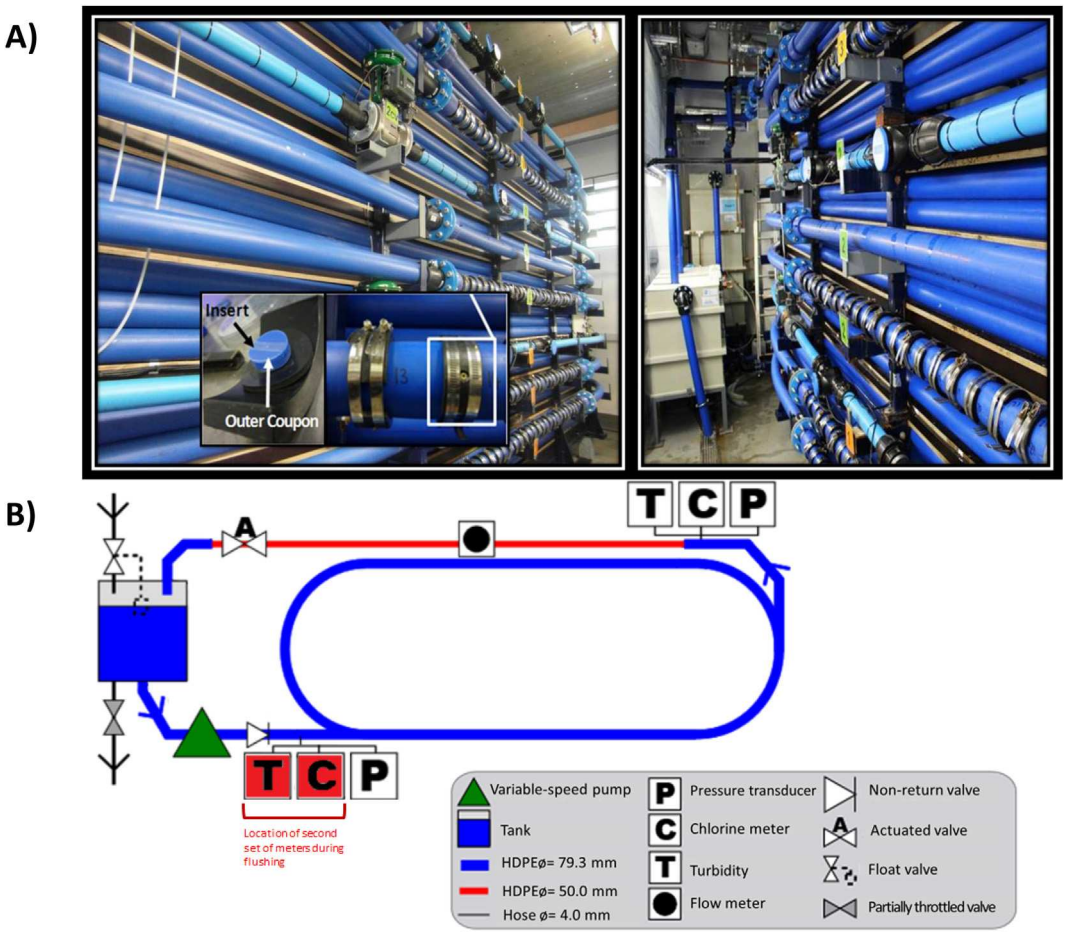


**Fig. 1.** A) Temperature controlled pipe-test facility at the University of Sheffield. PWG coupons were inserted along the length of each loop to allow for subsequent biofilm removal and examination. B) Schematic showing the characteristics of the loop used in this study to report biofilm development.

test for comparison of all time points and a Tukey and Kramer (Nemenyi) test for pairwise comparisons between two specific time points.

### 2.4. DNA extraction

To extract biofilm DNA from the coupons, the outer area of each coupon was brushed to remove biofilm following the procedure used by Deines et al. (2010). After brushing, biofilm suspensions were concentrated by filtering through 0.22-μm nitrocellulose membrane filters (Millipore, Corp.) as previously explained (Douterelo et al., 2013). Biofilm samples taken over the course of the experiment (n = 18) were then preserved in the dark at −80 °C until DNA was extracted. To extract DNA, a method based on proteinase K digestion followed by a standard phenol/chloroform/isoamyl alcohol extraction was used (Neufeld et al., 2007).

### 2.5. Q-PCR

Real-time PCR was used to quantify changes in the number of bacterial 16S and fungal ITS gene copies over time (see Table 1 for primer details). Quantification of samples involved the use of internal standard curves prepared by using a serial dilution of each targeted gene amplified from biofilm samples obtained from a previous experiment in the same test loop facility. For each gene, a standard was generated by running PCRs using the primers in Table 1 then purifying via gel-purification (Qiagen Gel-Extraction Kit) and combining the purified amplicons into one "DWDS biofilm" standard per gene. The number of gene copies in each standard was determined by quantifying the DNA content via a Nanodrop 8000 Spectrophotometer (Thermo Scientific, UK) and calculating gene copies using the equation:

Gene number = 6.023 × 1023 (copies mol-1) × concentration of standard (g μl-1) MW (g mol-1).

Where: 6.023 × 1023 is Avogadro's constant, MW is the molecular weight of the targeted gene.

Standards, no template controls and samples were amplified (in triplicate) via qPCR reactions according to the QuantiFast SYBR Green PCR kit (Qiagen, UK). Briefly, qPCR reactions were 25 μl in total volume, which contained 12.5 μl of QuantiFast® SYBR® Green PCR MasterMix, 9 μl of nuclease-free water (Ambion, Warrington, UK), 1.25 μl of each primer (10 μM; Table 1) and 1 μl of DNA template. Real-time PCR was carried out using an Applied Biosystems StepOne qPCR machine and the cycling conditions advised in the Qiagen kit (95 °C for 5 min, then 35 cycles of: 95 °C for 10 s, 60 °C for 30 s, melting curve analysis was also run for bacterial gene qPCRs only), the number of gene copies was determined using the StepOne software.

### 2.6. Illumina sequencing

Sequencing was performed by Illumina MiSeq technology with

**Table 1**
Primer pairs used for the q-PCR.

| Gene target (organisms) | Primer Pair | Primer sequences (5' – 3') | Primer reference |
|---|---|---|---|
| 16S rRNA | Eub338 | ACTCCTACGGGAGGCAGCAG | Lane, 1991 |
| (bacteria) | Eub518 | ATTACCGCGGCTGCTGG | Muyzer et al., 1993 |
| ITS (fungi) | ITS1F | TCCGTAGGTGAACCTGCGG | Gardes and Bruns, 1993 |
| | 5.8S | CGCTGCGTTCTTCATCG | Vilgalys and Hester 1990 |

the paired-end protocol by Mr DNA Laboratory (TX, USA) using primers 28F (GAGTTTGATCNTGGCTCAG) and 519 (RGTNTTACNGCGGCKGCTG) and the fungal 18S rRNA gene was amplified using SSUfungiF (TGGAGGGCAAGTCTGGTG)/SSUFungiR (TCGGCATAGTTTATGGTTAAG) (Hume et al., 2012).

Paired-end reads were merged and de-noised to remove short sequences, singletons, and noisy reads. Chimeras were detected using UCHIME (Edgar et al., 2011) and removed from further analysis. Sequences were clustered in Operational Taxonomic Units (OTUs) and selected using UPARSE (Edgar, 2013). Taxonomic assignments were made with USEARCH global alignment program (Edgar, 2013). The software PAST v3.12 (Hammer et al., 2008) was used to estimate Alpha-diversity at 97% sequence similarity and the Shannon diversity index, Chao-I and Dominance-H were calculated. Briefly, the Shannon index (H) measures diversity and indicates the proportion of OTUs abundance to the whole community, this index varies from 0 for communities with only a single taxon to higher values (max < 5 in this study). Chao 1, is an estimate of total richness and estimates total number of OTUS in a community based upon the number of rare OTUs found in a sample (Chao, 1984). In a sample with many singletons, the probability of having more undetected OTUs is higher, and the Chao 1 index will estimate greater richness than for a sample without rare OTUs. The evenness of a sample is a measure of the distribution of the OTUs in a community, and communities dominated by one or few OTUs have low evenness. The Dominance index (1-Simpson index) ranges from 0 (all taxa are equally present) to 1 (one taxon dominates the community completely) (Harper, 1999). Approximate confidence intervals for these indexes were computed with a bootstrap procedure (default 9999) and a 95% confidence interval was then calculated.

Bray Curtis dissimilarity matrixes at 97% sequence similarity cut off were calculated and visualised using non-metric multi-dimensional scaling (MDS) diagrams generated using the software PAST v3.12 (Hammer et al., 2008). Stress of the non-metric MDS was determined to estimate the statistical fit; stress varies between 0 and 1, with values near 0 indicating better fit.

The analysis of group similarities (ANOSIM) was performed based on Bray–Curtis dissimilarity distance matrices to test the differences in community composition among groups of samples using the software Primer6 (Clarke and Warwick, 2005). From this analysis gobal-R statistic values were calculated showing the strength of the impact that the factors analysed had on the samples, in this case time (days). Global-R values vary between 0 and 1, where 1 indicates high separation of the samples between levels of the factor (time) and 0 indicates no separation.

### 2.7. Statistical analysis of microbiological parameters and key taxonomic groups

Correlations between microbiological parameters were explored by Spearman's rank non parametric correlations using SPSS Statistics 24 (IBM, USA). Alpha-diversity metrics, the relative abundance of the most representative taxonomic class and the measurement of cells and genes for bacteria and fungi respectively were used as biological parameters in the establishment of correlations.

## 3. Results

### 3.1. Water physico-chemical analysis

As shown in Table 2 pH values were near neutral (7.08–7.99) for all the samples over time. Temperature ranged between 14.6 and 15.9 °C for all samples, within an average of 15 ± 0.4 °C. Free chlorine levels were slighted elevated on Day 0. This was due to initial filling of the system with fresh water that has a slightly higher residual than is ultimately established with the 24 h residence time from the trickle drain and feed, and the use of an elevated residual over night from cleaning to the start of the experiment. This elevated value was less than the final water quality leaving the local water treatment works, and dropped to the experimental level within 24 h. The average chlorine residual in the system was then maintained at 0.42 ± 0.2 mg/l.

Higher turbidity levels were observed on Day 0 (1.51 NTU) but subsequently were consistently at an average of 0.05 ± 0.03 NTU, this slight elevation is again associated with the filling of the system and upstream effects from the external network supplying the laboratories. TOC values were stable over time ranging from 1.13 to 1.83 mg/l. Iron was the physico-chemical factor that fluctuated the most, with minimum values of 9.9 μg/l on Day 34 to a maximum of 37.0 μg/l on Day 84. Manganese levels were very low over time, generally below detection limits (<3.6 μg/l) except for Day 14 which was 0.1 μg/l higher.

### 3.2. Volume and spread of cells

Fig. 2 shows the volume and spread of cells within the DWDS biofilms over the 84-day period. Note that Fig. 2A and B are the

**Table 2**
Average of physico-chemical parameters measured during every sampling event (n = 3) and standard deviation. TOC (total organic carbon); Fe (iron); Mn (manganese).

| | pH | T (°C) | Free Chlorine (mg/l) | Turbidity (NTU) | TOC (mg/l) | Fe (μg/l) | Mn (μg/l) |
|---|---|---|---|---|---|---|---|
| Day 0 | 7.46 ± 0.04 | 14.60 ± 0.00 | 0.98 ± 0.06 | 1.51 ± 0.05 | 1.13 ± 0.04 | 18.00 ± 0.81 | <3.6 ± 0.00 |
| Day 14 | 7.42 ± 0.37 | 14.70 ± 0.10 | 0.43 ± 0.01 | 0.08 ± 0.00 | 1.30 ± 0.08 | 21.00 ± 1.41 | 3.7 ± 0.00 |
| Day 34 | 7.61 ± 0.17 | 14.83 ± 0.00 | 0.43 ± 0.02 | 0.05 ± 0.00 | 1.37 ± 0.09 | 9.90 ± 0.00 | <3.6 ± 0.00 |
| Day 42 | 7.12 ± 0.15 | 15.03 ± 0.20 | 0.44 ± 0.03 | 0.04 ± 0.00 | * | 18.33 ± 2.62 | <3.6 ± 0.00 |
| Day 52 | 7.99 ± 0.31 | 15.20 ± 0.20 | 0.36 ± 0.01 | 0.05 ± 0.00 | 1.17 ± 0.04 | 14.33 ± 0.93 | <3.6 ± 0.00 |
| Day 70 | 7.07 ± 0.20 | 15.90 ± 0.10 | 0.42 ± 0.00 | 0.05 ± 0.00 | 1.33 ± 0.00 | 17 ± 0.00 | <3.6 ± 0.00 |
| Day 84 | 7.49 ± 0.22 | 15.03 ± 0.40 | 0.39 ± 0.05 | 0.06 ± 0.00 | 1.83 ± 0.11 | 37 ± 0.00 | <3.6 ± 0.00 |

* No measure was obtained

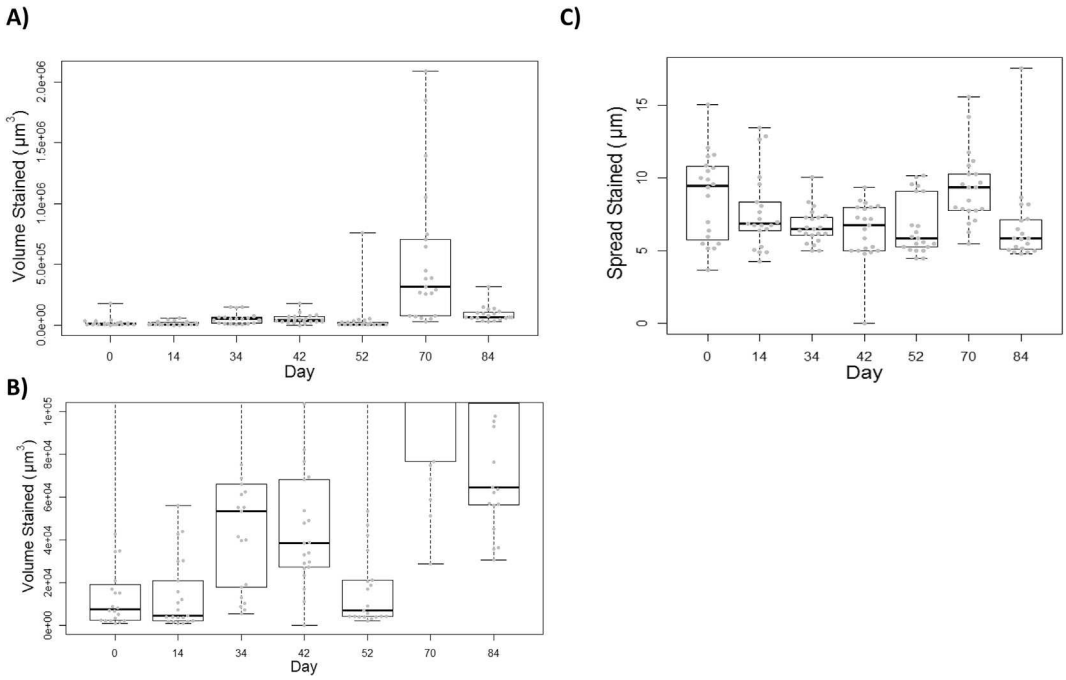


**Fig. 2.** Confocal analysis of biofilm cell development over time (n = 21). A) showing cell volume without data outliers, B) reduced Y-axis scale to appreciate differences in cell volume at first stages of biofilm development C) graph showing results from cell spread on coupons. (n = 21, in all cases apart from Day 0 where n = 20 and Day 82 where n = 19). In all cases box and whisker plots show the entire range of the data, the inter-quartile range and the median.

same data plotted on different vertical scales in order to visualise the variability of all the samples over the 3 months studied. As anticipated, the cell volume within the DWDS biofilms increased from Day 0 throughout the experiment as the biofilm developed (Fig. 2A) and significant difference were observed among data time points (Kruskall Wallis, $\chi^2 = 80.80$, P-value< 0.01). This increase in the cells volume was not linear, rather the volume oscillates with cell volume dropping at Day 52 to volumes comparable to those seen at Day 14 (Fig. 2B). However, no significant differences were detected using the pairwise comparison Nemeyi test among Day 52 and any other time points. Following this reduction in cells, the final two sample points (Day 70 and 84) have the greatest median cell volume (Fig. 2A and B) although Day 70 biofilms had a greater cell volume than Day 84.

Fig. 2C shows the 'spread' metric calculated from the biofilm CLSM data. Spread was calculated as volume divided by area covered (Fish et al., 2015), to provide a measure of spread or compactness of the biofilm, irrespective of the total volume and uncertainty in defining the edges of the distribution across the z-stack. While the trends, when all time points are compared, were statistically significant (Kruskal-Wallis, $\chi^2 = 26.411$, p-value < 0.05) it is notable that the data shows again an oscillating pattern. This pattern appears to be inverse and slightly lagged behind the volume data. When time points were compared pairwise, statistically significant differences (Nemeyi test, p-value < 0.05) were observed only between Day 70 samples and the other sampling days with the exception of Day 0 and Day 14.

### 3.3. Bacterial and fungal gene quantification

The number of bacterial 16S rRNA gene copies (Fig. 3A) increased from Day 0 (no genes were quantified) to Day 42 reaching a maximum of $1.16 \times 10^7$ 16S rRNA gene copies $mm^{-2}$. After Day 42 the number of gene copies decreases steadily over the rest of the experiment, despite this decline the Day 84 samples had a greater number of 16S rRNA genes than the Day 14 samples.

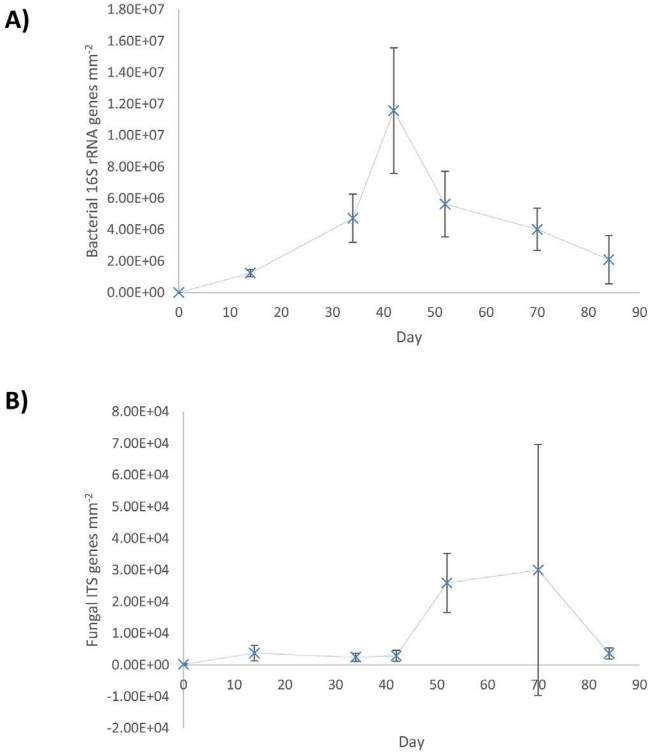


**Fig. 3.** Quantitative-PCR showing the number of genes per mm2 of biofilm over time for the A) 16S rRNA gene for bacteria and B) ITS gene for fungi.

Throughout the 84 day period the fungal ITS gene (Fig. 3B), was present at least two magnitudes less than the bacterial gene was. ITS genes $mm^{-2}$ were <10000 in biofilms from Days 0–42, by Day

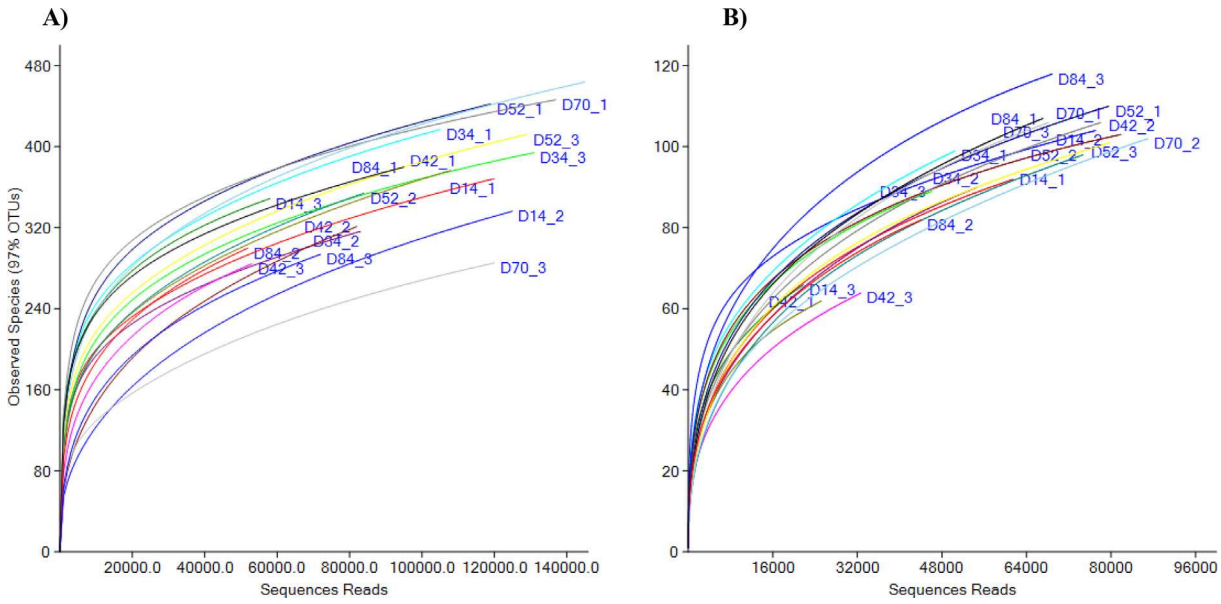


**Fig. 4.** Rarefaction analysis of microbial communities at 97% sequence similarity cut off, consider as species level for; A) bacteria and B) fungi. Numbers indicate the day of sampling (D14, D34, D42, D52, D70, D84) and the biological replicate (1, 2, 3).

52 gene copies had increased reaching a peak at Day 70 (max. 30000 ITS genes $mm^{-2}$). This pattern highlights a lag of 20–30 days in the fungi population reaching the maximum quantification in comparison to the bacteria where a peak was reached at Day 42. Similarly, to the bacteria, fungal gene copies decreased after this peak but the Day 84 biofilms had similar ITS gene copies as the Day 14 samples.

If the lagged growth and decline trends in bacteria and fungi (Fig. 3A and B) gene copies are combined, with some weighting for relative size of organism, it is possible that the cyclic trend in DNA cellular volume (Fig. 2A and B) could be explained.

### 3.4. Microbial community structure

#### 3.4.1. Rarefaction analysis

The rarefaction analysis (Fig. 4) yields insights into the sequencing effort and compares the diversity of the observed number of OTUs at 97% sequence similarity cut off in all the samples over time. Most of the samples, independently of the time of sampling, showed rarefaction curves that did not reach a plateau. This trend in the curves was particularly marked for fungal communities (Fig. 4B), where the samples analysed showed a steeper slope when compared with bacteria, suggesting that further

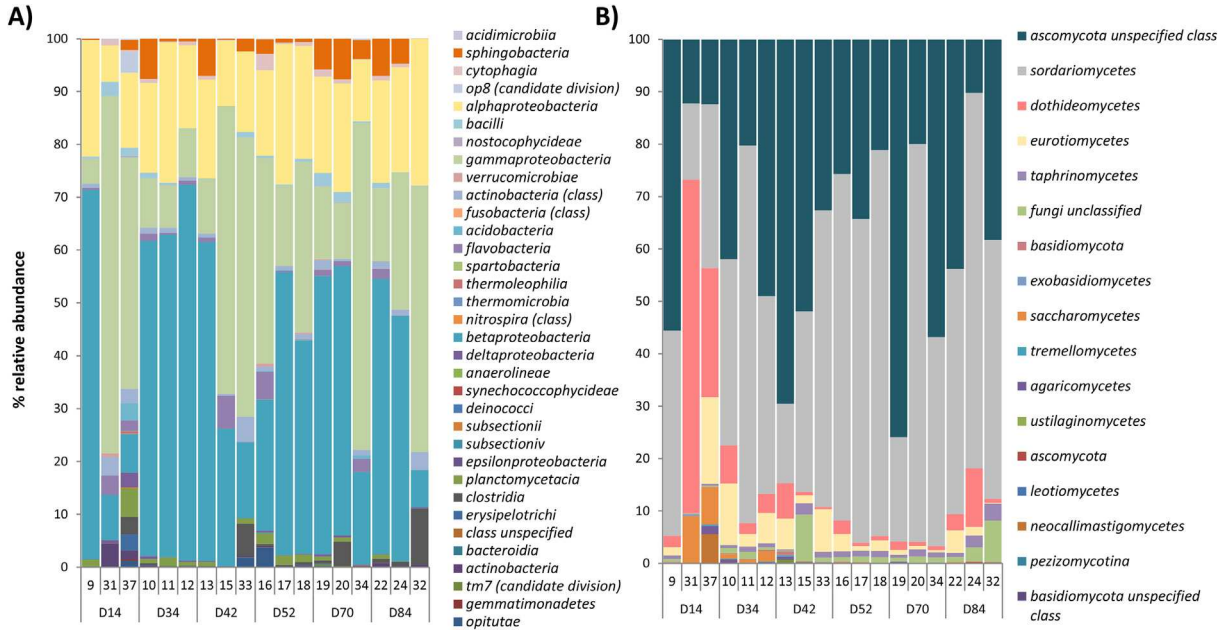


**Fig. 5.** Temporal changes in the microbial community structure over time at class level for A) bacteria and B) fungi. Numbers within each sampling day (D14, D34, D42, D52, D70 and D84) indicates the number of the coupon sampled.

sequencing and time series would be needed to reach a full taxonomic representation of the microbial communities. This data can also be associated to the fact that biofilm communities did not reach a mature or stable state after three months of development in the system.

### 3.4.2. Taxonomic analysis

The dominant bacterial class (Fig. 5A) over time in the biofilm samples was *Proteobacteria* and within it *Betaproteobacteria* (representing a 70% of the total community on Day 34 samples), *Gammaproteobacteria* (5–67%) and *Alphaproteobacteria* (6–28%) were the most abundant classes. However, the percentages of each of these bacterial classes clearly varied over time and there was high variability between replicates for each day, with Day 14 having the most extreme example of this. The fungal community (Fig. 5B) was dominated by *Ascomycota* (10–75%) and *Sordaryomicetes* (14–75%) but Day 14 samples from two coupons (31 and 37) were dissimilar to the other samples and were dominated by *Dothideomycetes* (22–63%) and *Saccharomyctes* (yeast and yeast like –fungi, 7–9%). *Saccharomycetes* were dominant in the first stages of biofilm development until Day 42, and then this fungal group was not substantially represented in the community.

At genus level (Fig. 6A), *Massilia* (max. 62%) and *Pseudomonas* (max. 64%) were highly abundant on the first days of biofilm development. It is notable that on Day 14, one of the replicates (coupon 9) showed a different microbial community when compared with the other two samples despite of being biological replicates. These two samples from Day 14 had a higher relative abundance of *Pseudomonas* (38–64%), this genus was dominant in the community composition and showed percentages similar to

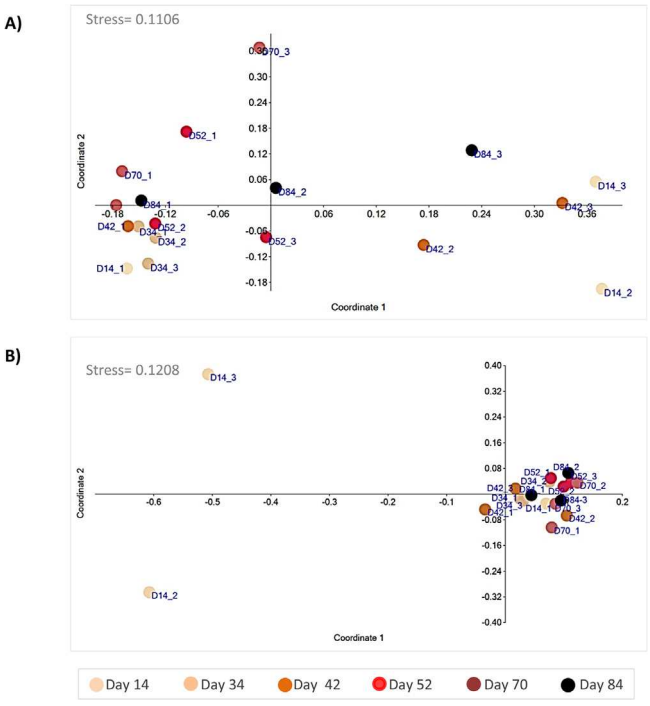


**Fig. 7.** Nonmetric multidimensional scaling plot of biofilm samples (n = 18) from various sampling times (days). The analysis was based on Bray–Curtis similarity matrix calculated from the relative abundance of OTUs at 97% sequence similarity cut off. A) bacteria and B) fungi.

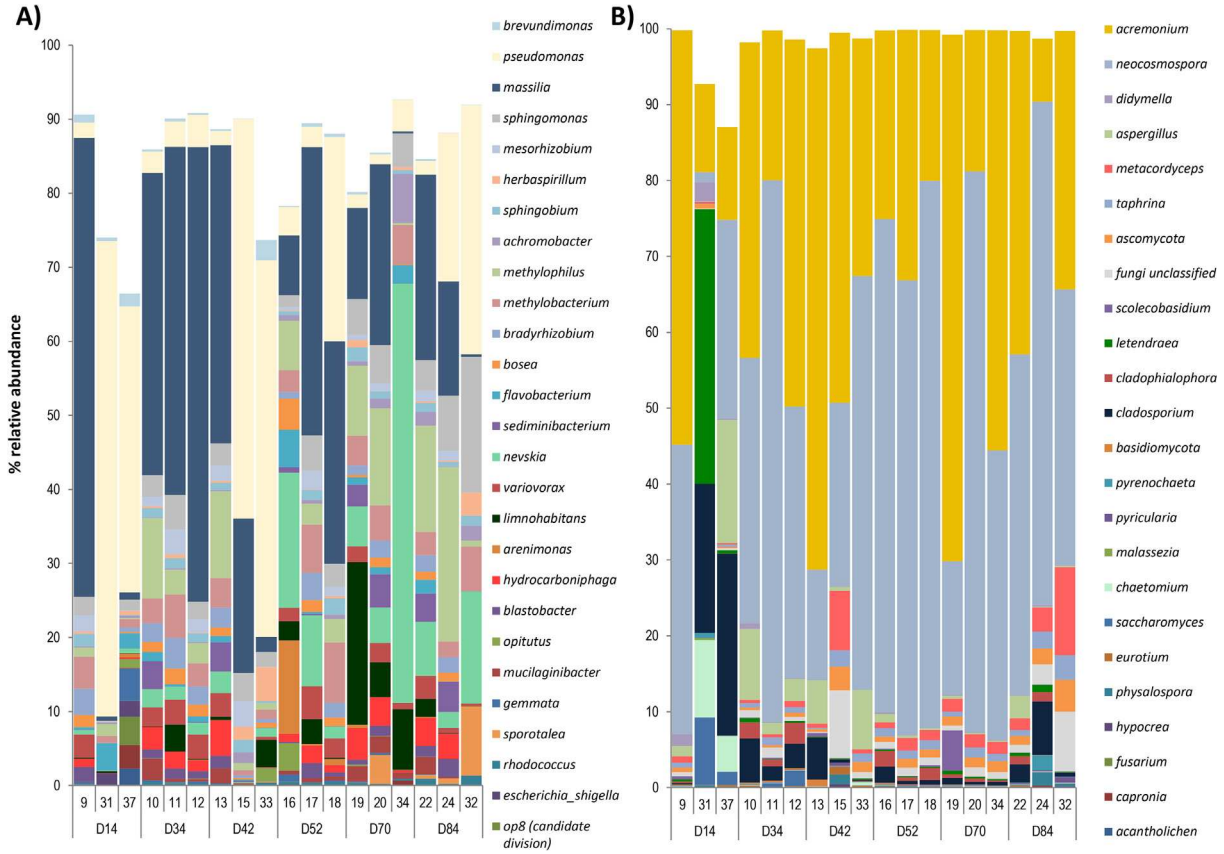


**Fig. 6.** Analysis of microbial community data at genus level, showing the relative abundance of the most abundant genera inhabiting biofilms A) bacteria B) fungi. Numbers within each sampling day (D14, D34, D42, D52, D70 and D84) indicates the number of the coupon sampled.

those on Day 42.

On Day 42, samples showed a more diverse community enriched (coincident in time with a peak in the cell volume, Fig. 2 A and B) with genera such as *Nevskia*, *Methylophilus*, *Sphingomonas*, *Variovorax* and *Limnohabitants*. The most abundant genera in fungal communities (Fig. 6B) at all sampling times were *Acremonium* (8–70%) and *Neocosmospora* (17–77%) but in two of the coupons from Day 14 (31 and 37) there was high abundance of *Letendraea* (36%) and *Cladosporium* (19–24%). The fungal composition of these two samples was markedly different when compared with the most even structure observed for the samples at other time points. This has been also observed, as has been previously pointed, for the bacterial communities of these two samples. The studied succession finished with samples from Day 84 showing a high abundance of the genus *Metacordyceps* in the fungal community (2–12%).

MDS analysis of bacteria (based on the Bray-Curtis similarity matrix of bacterial sequences with 97% similarity cut off) is presented in Fig. 7A. Variability in bacterial community distribution between sample points was observed but these differences were not significant (ANOSIM: global-R = 0.143 p-value = 0.074) and there was no clear temporal pattern. For fungi (Fig. 7B) the MDS analysis revealed a tight clustering of the biofilm samples, which corresponds to very little variation in community composition over time as shown in the ANOSIM analysis (R = 0.023, p-value = 0.399).

### 3.4.3. Diversity and richness indicators

Fig. 8 shows the richness (i.e. number of different OTUs) and diversity (i.e. number of different OTUs taking into account their relative abundance) of bacterial and fungal communities at 97% sequence similarity cut off. When compared, bacterial communities were more dynamic and diverse than fungi; fungal communities showed limited diversity, dominated by few taxonomic groups with little change over time. When analysed separately, the dominance indicator for bacterial communities decreased over time, increasing slightly by Day 70 and decreasing again by Day 84, reaching a minimum value. This trend suggests that initially there

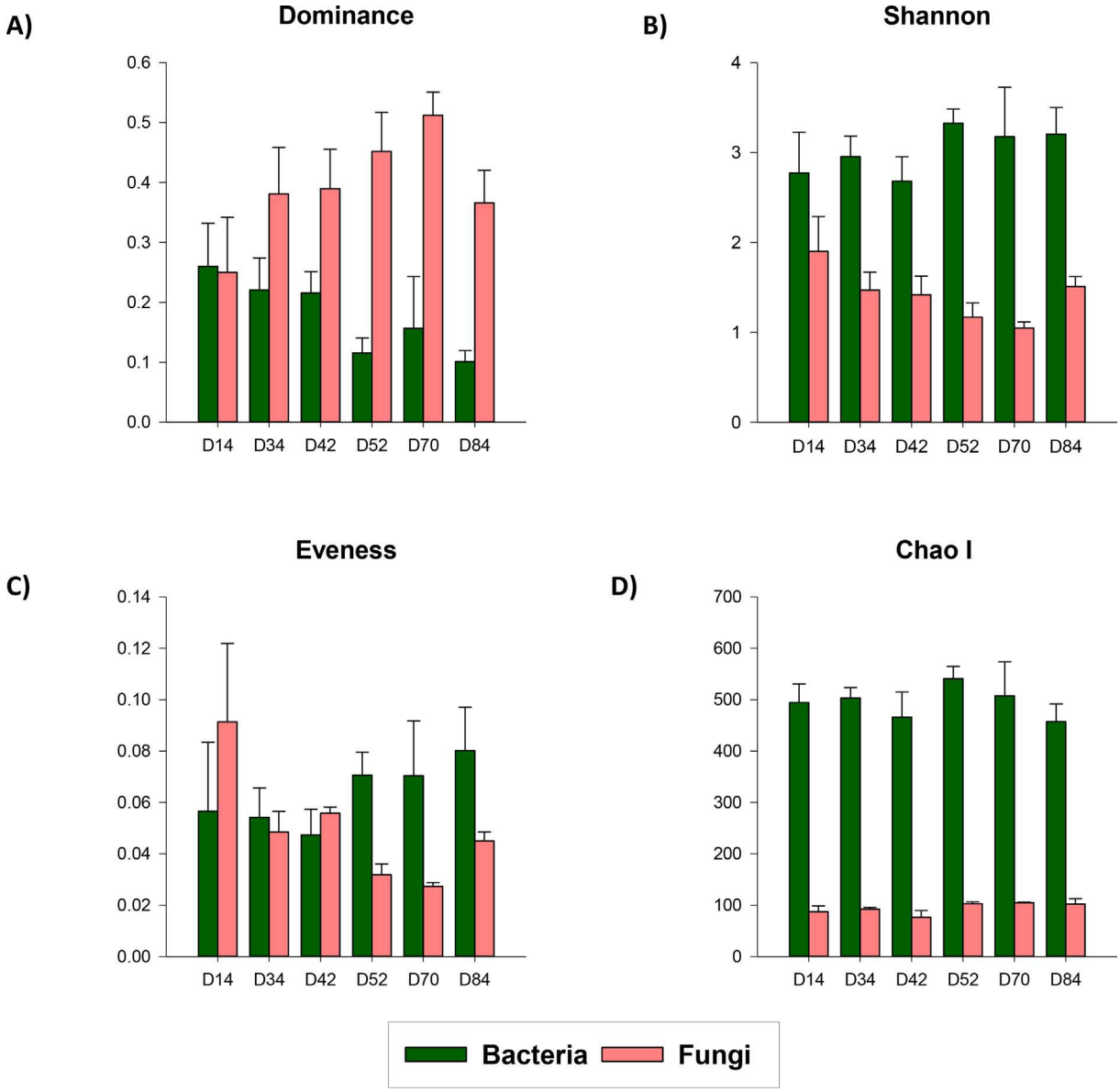


**Fig. 8.** Result for A) dominance, B) diversity (Shannon), C) evenness and D) Chao I indexes for bacteria and fungi at 97% sequence similarity cut off over time. Bars indicate standard deviation (n = 3).

**Table 3**
Matrix showing results of the non-parametric correlations between the microbiological parameters analysed in this study.

| | Chao 1 B | Shannon B | Chao 1 F | Shannon F | Genes 16S /mm2 | Genes ITS/mm2 | Mediam cell volume | Betaproteobacteria | Alphaproteobacteria | Gammaproteobacteria | Planctomycetacia |
|---|---|---|---|---|---|---|---|---|---|---|---|
| Shannon B | **.513*** | 1.000 | | | | | | | | | |
| Chao 1 F | -0.012 | -0.045 | 1.000 | | | | | | | | |
| Shannon F | -0.302 | -0.181 | 0.084 | 1.000 | | | | | | | |
| Genes 16S /mm2 | 0.047 | -0.078 | -0.216 | -0.254 | 1.000 | | | | | | |
| Genes ITS/mm2 | 0.292 | 0.266 | **.455*** | **-.442*** | -0.257 | 1.000 | | | | | |
| Mediam cell volume | -0.066 | 0.223 | 0.311 | -0.254 | -0.029 | 0.086 | 1.000 | | | | |
| *Betaproteobacteria* | **.728**** | 0.224 | -0.193 | **-.472*** | 0.129 | -0.028 | 0.185 | 1.000 | | | |
| *Alphaproteobacteria* | **.635**** | 0.271 | 0.060 | **-.728**** | 0.034 | 0.335 | 0.185 | **.744**** | 1.000 | | |
| *Gammaproteobacteria* | -0.307 | -0.259 | **.520*** | 0.257 | 0.009 | **.461*** | -0.047 | **-.641**** | **-.401*** | 1.000 | |
| *Planctomycetacia* | **.546**** | **.428*** | -0.326 | -0.349 | 0.094 | 0.251 | **-.489*** | 0.353 | **.475*** | -0.261 | 1.000 |
| *Actinobacteria* | -0.238 | -0.018 | -0.027 | 0.288 | -0.323 | 0.103 | -0.154 | **-.420*** | -0.284 | 0.375 | -0.065 |
| *Bacilli* | **.453*** | **.470*** | -0.081 | -0.042 | -0.317 | 0.367 | -0.034 | 0.170 | 0.098 | 0.096 | 0.344 |
| *Sphingobacteria* | **.418*** | **.639**** | -0.070 | -0.290 | 0.147 | 0.229 | **.505*** | 0.368 | 0.106 | -0.170 | 0.080 |
| *Clostridia* | 0.076 | **.627**** | -0.023 | -0.039 | -0.201 | 0.216 | 0.194 | -0.169 | 0.077 | 0.049 | 0.088 |
| *Actinobacteria* | -0.203 | 0.150 | 0.123 | **.428*** | -0.386 | 0.135 | -0.254 | **-.531*** | **-.441*** | **.422*** | -0.006 |
| *Cytophagia* | **.610**** | **.449*** | 0.258 | 0.015 | -0.060 | 0.342 | 0.072 | 0.399 | 0.245 | 0.158 | 0.269 |
| *Ascomycota* | 0.230 | -0.148 | 0.185 | -0.185 | 0.129 | 0.160 | 0.354 | 0.344 | 0.379 | -0.079 | -0.144 |
| *Sordariomycetes* | 0.038 | 0.075 | **.477*** | **-.558**** | 0.129 | 0.335 | 0.223 | 0.038 | **.437*** | 0.100 | 0.074 |
| *Dothideomycetes* | 0.220 | 0.257 | 0.017 | **.449*** | **-.430*** | -0.116 | -0.223 | 0.117 | -0.220 | -0.156 | 0.086 |
| *Taphrinomycetes* | -0.115 | -0.011 | **.614**** | -0.321 | 0.160 | 0.285 | 0.348 | -0.123 | 0.311 | 0.249 | -0.145 |
| *Basidiomycota* | **.466*** | 0.089 | -0.050 | -0.219 | 0.329 | -0.342 | 0.000 | **.677**** | **.512*** | **-.630**** | **0.273** |
| *Saccharomycetes* | 0.019 | 0.183 | -0.028 | **.480*** | **-.408*** | -0.223 | -0.220 | -0.018 | -0.197 | -0.145 | 0.166 |
| *Leotiomycetes* | 0.082 | -0.036 | **.514*** | -0.116 | 0.189 | 0.186 | 0.396 | 0.274 | **.405*** | 0.096 | -0.141 |

* Correlations are significant at 0.05 level (1- tailed), **Correlations are significant at 0.01 level (1- tailed).

are a few bacteria that attach and colonize the pipe surfaces, from which the biofilm develops towards a more diverse community, with less dominating taxa. This is supported by the patterns in diversity, evenness and richness values. However, bacterial richness indicator did not change considerably over time. Fungal communities showed a clear dominance of certain OTUs, which was less marked at the beginning of the data series studied and increased over time. Similarly, evenness was higher for the first 42 days of biofilm development and subsequently fluctuated at lower level after that day. The fungal communities were not very diverse with all samples having Shannon index values below 2. Richness (<100 OTUs) fluctuated only slightly among samples. Clearly, few fungal OTUs dominated the composition of biofilms over time.

### 3.5. Correlations between microbiological data

Table 3 shows a matrix of the non-parametric correlations between microbiological data and indicates statistically significant correlations at different p-levels. The diversity and richness indicators showed a significant positive correlation for bacteria but not for fungi. Only the number of fungal ITS genes correlated significantly with richness and diversity for that taxonomic group. The cell volume did not significantly correlate with any of the other parameters. When associations between different microbial groups were taken into account, *Alphaproteobacteria* and *Betaproteobacteria* tended to be correlated positively among them. The microbial groups that correlated the most with other microorganisms were the bacteria *Actinobacteria, Cytophagia* and the fungi *Dothideomycetes, Basiodioycota, Leotiomycetes* and *Ascomycota*. This result shows that certain microbial groups are more or less likely to coexist within the studied biofilm samples.

## 4. Discussion

Biofilm development was monitored over a three-month period and the characteristics of inter-taxa interactions were studied to evaluate and detect patterns of temporal change and drivers of biofilm behaviour. Sequencing results indicated that biofilm developmental patterns were initially driven by bacteria. Fungi showed a lag response to temporal changes in terms of ITS gene copy numbers and the community structure displayed limited changes over time. Generally, it was observed that an initial, diverse community (dominated by bacteria) was able to attach and was embedded in the biofilm. After one month of development, biofilm diversity was temporally reduced, coincident with a decrease in cell volume from Days 42–52, likely due to a selective mechanism that ultimately yielded a higher diversity after two months development. Confirming the leading role of bacteria in the process of succession it was observed that the rise in diversity from 34 to 42 days, corresponded with a peak in the number of 16s rRNA gene copy numbers. The observed diversity pattern could have been a result of competition, with some bacteria/fungi being outcompeted (hence diversity decreasing) but the resultant more mature biofilm then being a suitable niche for other cells to subsequently colonize (hence diversity increasing again). We hypothesize that the daily fluctuating hydraulic conditions were acting as a selective mechanism to shape microbial diversity and structure, as has been previously observed in previous research carried out in the same system (Douterelo et al., 2013; Fish et al., 2017). If daily patterns help to maintain natural diverse communities and more compact and stable biofilms, this can have positive implications for the management of DWDS, safeguarding these systems from the incursion of non-desirable microorganisms into biofilms and avoiding their survival and later mobilisation into bulk water.

The ability of microorganisms to respond to changing environmental conditions has been previously correlated with the bacterial genome size and with their cell volume (Yooseph et al., 2010). Here the dominant peak in cell volume (Day 70 on Fig. 2A) corresponded to the peak in ITS gene numbers (Fig. 3B) which can be explained by the generally larger cell size of fungi, particularly of filamentous fungi when forming hyphae. If this hypothesis is correct, fungi may be more resilient to change and persist over time, explaining the limited change in diversity observed during the succession process and the observed lag between the peak in bacteria and fungi genes apparent when comparing Fig. 3A and B. Fungi can survive and grow in DWDS within biofilms, particularly at warmer temperature or in systems where the flow is low or stagnant (Siqueira et al., 2012; Douterelo et al., 2016b; Oliveira et al., 2016). The night time

| Actinobacteria | Bacilli | Sphingobacteria | Clostridia | Actinobacteria | Cytophagia | Ascomycota | Sordariomycetes | Dothideomycetes | Taphrinomycetes | Basidiomycota | Saccharomycetes |
|---|---|---|---|---|---|---|---|---|---|---|---|
| 1.000 | | | | | | | | | | | |
| **.525*** | 1.000 | | | | | | | | | | |
| -0.123 | **.455*** | 1.000 | | | | | | | | | |
| 0.390 | 0.354 | 0.305 | 1.000 | | | | | | | | |
| **.715**** | **.422*** | -0.018 | 0.292 | 1.000 | | | | | | | |
| 0.034 | **.593**** | **.470*** | 0.051 | 0.255 | 1.000 | | | | | | |
| -0.176 | -0.220 | -0.011 | -0.266 | **-.432*** | -0.141 | 1.000 | | | | | |
| **-.414*** | -0.273 | -0.046 | 0.116 | -0.179 | -0.065 | -0.022 | 1.000 | | | | |
| 0.092 | 0.354 | 0.226 | -0.070 | **.420*** | **.575**** | **-.482*** | **-.418*** | 1.000 | | | |
| -0.383 | **-.484*** | -0.187 | 0.139 | -0.327 | -0.245 | 0.271 | **.835**** | **-.587**** | 1.000 | | |
| **-.466*** | -0.265 | 0.089 | -0.336 | **-.411*** | 0.222 | 0.159 | 0.069 | 0.229 | -0.032 | 1.000 | |
| 0.058 | 0.281 | -0.147 | -0.149 | **.403*** | 0.382 | -0.320 | -0.227 | **.592**** | -0.377 | 0.032 | 1.000 |
| -0.372 | **-.460*** | -0.076 | -0.147 | **-.410*** | 0.145 | **.607**** | 0.283 | -0.236 | **.589**** | 0.326 | -0.191 |

flow rate of the hydraulic regime selected for these experiments was at the upper end for those observed in 75–100 mm pipes in real systems, thus fungi are possibly even more prevalent and important in real operational systems. The challenge for water utilities is how to manage/control these microorganisms since fungal walls protect cells against mechanical damage and stop the ingress of toxic molecules, making these organisms even more resistant to environmental changes (Cole, 1996). In addition, fungi can form spores which increase their resistance to disinfection (Mamane-Gravetz and Linden, 2005; Sonigo et al., 2011). This study reinforces that fungi must be included in monitoring campaigns in DWDS when assessing microbial risks.

It has been suggested that, generally, microbial communities tend to develop towards a stable community (Faust et al., 2015) or plateau phase. In this study, no mature/stable biofilm communities were established on the pipe walls after three months of development. This result suggests that longer time periods may be needed to fully develop mature microbial communities in DWDS. However, determining the scale of change to study succession in an ecosystem is challenging, given that depending on the habitat, community changes can be triggered by fluctuations in environmental conditions or by a transient perturbation that moves the system into an alternative steady state (Fierer et al., 2010). The experimental DWDS used in this study minimised any such transient perturbations, by controlling hydraulics and offering a relatively stable physico-chemical environment over time. While the local source water, treatment works and trunk main system prior to the laboratory facility will have had some variations over the 3 months, Table 2 indicates that these where minimal and they would have been gradual fluctuations rather than rapid dynamic changes. Hence the changes observed such as those on Day 42 are most probably due to intrinsic biofilm processes, related to microbial processes during development. Martiny et al. (2003) studied the process of biofilm development over a 3-year period in a model distribution systems using fingerprinting and Sanger sequencing to monitor bacterial communities. Using these methods, Martiny et al. (2003) established that after 500 days, the biofilm entered a stable state, which was characterised by a greater richness of bacteria. We have observed higher bacterial diversity at the final stages of biofilm formation but after three months of biofilm development our communities were not mature or stable.

We have observed that specific microbial taxa were dominant throughout the succession process with a core microbial population present in the biofilms over time but at different relative abundances. Thus, it can be suggested that these particular microbial taxa are fundamental in directing the process of succession. The taxa in this core community include the bacteria *Pseudomonas*, *Massillia* and *Sphingomonas* and the fungi *Acremonium* and *Neocosmopora*. In a previous study, the role of *Pseudomonas* as primary and initial colonizer of the same experimental facility was established in the first 28 days of biofilm development (Douterelo et al., 2014b) and here its continual key role in shaping biofilm structure over a longer period of time has been confirmed. Species belonging to the genus *Pseudomonas* might benefit from what is known as the founder effect, as an initial member of biofilms in the pipe surface it will have the advantage over secondary colonizers and will remain dominant over time (Kelly et al., 2014). The presence of core populations have been observed before in water meters of DWDS (Ling et al., 2016), biofilms of a chloraminated DWDS (Kelly et al., 2014) and in DWDS of chlorinated systems (Douterelo et al., 2017). Kelly et al., 2014 showed in chloraminated systems that the core community was enriched with methanotrophs and methylotrophs. *Methylobacteria* and *Methylophylus* were also important representatives of bacterial communities over time in this study and the relative abundance of *Methylophylus* increased after two months of biofilm development. Methylotrophic bacteria have been found in several drinking water-related ecosystems (McCoy and VanBriesen, 2012; Douterelo et al., 2014b; Liu et al., 2014b) but the reasons behind their abundance in these systems are unclear. However, methylotrophic bacteria have been related with the generation of holoacetic acid which is a common disinfectant by-product in chlorinated systems (Kelly et al., 2014), therefore it is possible that this group is promoted due to the decay of residuals within DWDS.

The fungi *Acremonium* and *Neocosmopora* were also forming part of the fungal-bacteria core community. *Acremonium* is a filamentous fungus which has been previously isolated in water supply reservoirs, drinking water treatment plants and in bulk water of drinking water distribution systems (Zacheus and Martikainen,

1995; Pereira et al., 2010; Oliveira et al., 2016; Bai et al., 2017; Douterelo et al., 2017) and has been associated with the occurrence of taste and odour issues in drinking water (Bai et al., 2017). *Neocosmopora* is commonly found in soils and some species are phytophatogenic (Aoki et al., 2014). It has been found that *Neocomospora*, under laboratory conditions is able to uptake chloride (Miller and Budd, 1975) and can produce cyclosporine a fungal metabolite with antifungal activity; these abilities can explain its supremacy over other microorganisms in mixed-species microbial communities in chlorinated DWDS. This study confirms the presence of *Acremonium* and *Neocomospora* from the early stages of biofilm formation to a more developed biofilm in chlorinated systems forming core communities with bacteria. Despite of fungi involvement in the organoleptic deterioration of water, act as potential pathogens and toxin producers, fungi are usually omitted from drinking water regulation and there are no limits or standards regarding their presence in drinking water. This study shows the ubiquity of fungi in forming mix-species consortium with the most common bacteria in DWDS biofilms. Taking into account these results, further consideration should be given to these microorganisms in order to guarantee the delivery of good quality water and to control biofilm formation at the initial stages of development in DWDS.

Environmental stressors such as chlorine, can influence successional trajectories in the early stages of succession (Fierer et al., 2010) by increasing the abundance of taxa that are resistant to the particular stress and can subsequently modify the habitat by producing EPS (extracellular polymeric substances) to protect the cells from oxidative stress (Besemer et al., 2007). This study indicates the capability of microorganisms to proliferate despite the presence of chlorine residual throughout biofilm development, from initial stages with low cell numbers and thinner and more environmentally exposed biofilms, to more developed biofilms exhibiting larger biomass and diversity. From these results, it can be hypothesised that the microbial communities involved in initial attachment to the pipes are more resistant to chlorine, then once more EPS is produced, other species which are less resistant can join the biofilm and survive within it protected against the action of chlorine by the EPS, hence the biofilm environment may favour more diverse communities over time. This suggests that, despite its widespread use to control planktonic microorgansims, the application of chlorine to control the attached microbial life within DWDS is questionable. In agreement with our observations, Simões et al. (2016) under controlled laboratory conditions, studied the role of interkingdom interactions in chlorine resistance and showed that associations between fungi and bacteria were ecologically beneficial and promoted resistance to disinfection.

The stable state of a biofilm is not entirely determined by external factors and interactions among microbial community members might play a key role in determining biofilm status (Faust et al., 2015). These complex interactions between microorganisms and with their environment are key contributors to biofilm dynamics and are relatively unexplored in the context of DWDS. Here the relative abundance of certain bacterial and fungal taxa correlated together including *Proteobacteria* and *Basidiomycota* (Table 3), both members of a core microbial community present continuously over the successional process in this study. Fungal-bacteria associations can lead to changes in nutrient availability, even in the case of DWDS where the level of nutrients such as TOC in the system are controlled to a certain extent. The presence of certain taxa can ease nutrient limitation and it is well known that in other ecosystems bacterial and fungal consortium are able to increase nutrient bioavailability and mobilisation of key nutrients (Rashid et al., 2016) and this can support the process of succession. However, if biofilms are to a certain extent self-sufficient, independently of the concentration of available nutrients in the bulk-water, manipulating or changing external nutrient parameters is not going to stop biofilm formation and development in DWDS.

## 5. Conclusions

- Diverse bacterial communities cohabiting with more stable fungal communities, with the more common taxa ubiquitous and constantly present over time and a temporal variability that does not follow a specific pattern driven by bacteria.
- To deal with the heterogeneity of the process of biofilm development in DWDS and to model these systems, the focus needs to be on targeting dominant and ubiquitous microorganisms.
- In order to manage microbial risks in DWDS we need to better understand the behaviour of these key microorganisms, to design monitoring strategies and assess their use as bioindicators of overall biofilm status in the system.

## Acknowledgements

The research reported here was supported by the UK Engineering and Physical Sciences Research Council (EPSRC). EPSRC-LWEC Challenge Fellowship EP/N02950X/1, the Challenging Engineering Grant EP/G029946/1 and the EPSRC Platform Grant Funding EP/1029346/1.

## References

Aoki, T., O'Donnell, K., Geiser, D.M., 2014. Systematics of key phytopathogenic Fusarium species: current status and future challenges. J. Gen. Plant Pathol. 80, 189–201.
Ashbolt, N.J., 2015. Microbial contamination of drinking water and human health from community water systems. Current environmental health reports 2, 95–106.
Bai, X., Zhang, T., Qu, Z., Li, H., Yang, Z., 2017. Contribution of filamentous fungi to the musty odorant 2,4,6-trichloroanisole in water supply reservoirs and associated drinking water treatment plants. Chemosphere 182, 223–230.
Besemer, K., Singer, G., Limberger, R., Chlup, A.K., Hochedlinger, G., Hodl, I., Baranyi, C., Battin, T.J., 2007. Biophysical controls on community succession in stream biofilms. Appl. Environ. Microbiol. 73, 4966–4974.
Buse, H.Y., Lu, J., Struewing, I.T., Ashbolt, N.J., 2013. Eukaryotic diversity in premise drinking water using 18S rDNA sequencing: implications for health risks. Environ. Sci. Pollut. Res. 20, 6351–6366.
Chao, A., 1984. Non parametric estimation of the number of classes in a population. Scand. J. Stat. 11, 265–270.
Chao, Y., Mao, Y., Wang, Z., Zhang, T., 2015. Diversity and functions of bacterial community in drinking water biofilms revealed by high-throughput sequencing. Sci. Rep. 5, 10044.
Clarke, K., Warwick, R., 2005. Primer-6 computer program. Natural Environment Research Council, Plymouth.
Cole, G.T., 1996. Basic Biology of Fungi.
Deines, P., Sekar, R., Husband, P.S., Boxall, J.B., Osborn, A.M., Biggs, C.A., 2010. A new coupon design for simultaneous analysis of in situ microbial biofilm formation and community structure in drinking water distribution systems. Appl. Microbiol. Biotechnol. 87, 749–756.
Douterelo, I., Boxall, J.B., Deines, P., Sekar, R., Fish, K.E., Biggs, C.A., 2014a. Methodological approaches for studying the microbial ecology of drinking water distribution systems. Water Res. 65, 134–156.
Douterelo, I., Jackson, M., Solomon, C., Boxall, J., 2016a. Microbial analysis of in situ biofilm formation in drinking water distribution systems: implications for monitoring and control of drinking water quality. Appl. Microbiol. Biotechnol. 100, 3301–3311.
Douterelo, I., Jackson, M., Solomon, C., Boxall, J., 2016b. Microbial analysis of in situ biofilm formation in drinking water distribution systems: implications for monitoring and control of drinking water quality. Appl. Microbiol. Biotechnol. 100, 3301–3311.
Douterelo, I., Jackson, M., Solomon, C., Boxall, J., 2017. Spatial and temporal analogies in microbial communities in natural drinking water biofilms. Sci. Total Environ. 581, 277–288.
Douterelo, I., Sharpe, R., Boxall, J., 2014b. Bacterial community dynamics during the early stages of biofilm formation in a chlorinated experimental drinking water distribution system: implications for drinking water discolouration. J. Appl. Microbiol. 117, 286–301.
Douterelo, I., Sharpe, R.L., Boxall, J.B., 2013. Influence of hydraulic regimes on bacterial community structure and composition in an experimental drinking water distribution system. Water Res. 47, 503–516.

Edgar, R.C., 2013. UPARSE: highly accurate OTU sequences from microbial amplicon reads. Br. J. Pharmacol. 10, 996–998.
Edgar, R.C., Haas, B.J., Clemente, J.C., Quince, C., Knight, R., 2011. UCHIME improves sensitivity and speed of chimera detection. Bioinformatics 27, 2194–2200.
Faust, K., Lahti, L., Gonze, D., de Vos, W.M., Raes, J., 2015. Metagenomics meets time series analysis: unraveling microbial community dynamics. Curr. Opin. Microbiol. 25, 56–66.
Fierer, N., Nemergut, D., Knight, R., Craine, J.M., 2010. Changes through time: integrating microorganisms into the study of succession. Res. Microbiol. 161, 635–642.
Fish, K., Osborn, A., Boxall, J., 2017. Biofilm structures (EPS and bacterial communities) in drinking water distribution systems are conditioned by hydraulics and influence discolouration. Sci. Total Environ. 593, 571–580.
Fish, K.E., Collins, R., Green, N.H., Sharpe, R.L., Douterelo, I., Osborn, A.M., Boxall, J.B., 2015. Characterisation of the physical composition and microbial community structure of biofilms within a model full-scale drinking water distribution system. PLoS One 10, e0115824.
Flemming, H.C., 1998. Relevance of biofilms for the biodeterioration of surfaces of polymeric materials. Polym. Degrad. Stabil. 59, 309–315.
Gardes, M., Bruns, T.D., 1993. ITS primers with enhanced specificity for basidiomycetes–application to the identification of mycorrhizae and rusts. Mol. Ecol. 2, 113–118.
Gomes, I.B., Simões, M., Simões, L.C., 2014. An overview on the reactors to study drinking water biofilms. Water Res. 62, 63–87.
Gomez-Alvarez, V., Pfaller, S., Revetta, R.P., 2016. Draft genome sequence of two sphingopyxis sp. Strains, dominant members of the bacterial community associated with a drinking water distribution system simulator. Genome Announc. 4.
Hammer, Ø., Harper, D., Ryan, P., 2008. PAST-palaeontological Statistics, Ver. 1.89. *Paleontological Museum. University of Oslo, Noruega* (También disponible en línea: http://folk.uio no/ohammer/past/index.html).
Harper, D.A.T.e, 1999. Numerical Palaeobiology. John Wiley & Sons.
Hoefel, D., Monis, P.T., Grooby, W.L., Andrews, S., Saint, C.P., 2005. Profiling bacterial survival through a water treatment process and subsequent distribution system. J. Appl. Microbiol. 99, 175–186.
Hume, M.E., Hernandez, C.A., Barbosa, N.A., Sakomura, N.K., Dowd, S.E., Oviedo-Rondón, E.O., 2012. Molecular identification and characterization of ileal and cecal fungus communities in broilers given probiotics, specific essential oil blends, and under mixed Eimeria infection. Foodb. Pathog. Dis. 9, 853–860.
Husband, P.S., Boxall, J.B., Saul, A.J., 2008. Laboratory studies investigating the processes leading to discolouration in water distribution networks. Water Res. 42, 4309–4318.
Husband, S., Fish, K.E., Douterelo, I., Boxall, J., 2016. Linking discolouration modelling and biofilm behaviour within drinking water distribution systems. Water Sci. Technol. Water Supply.
Kelly, J.J., Minalt, N., Culotti, A., Pryor, M., Packman, A., 2014. Temporal Variations in the Abundance and Composition of Biofilm Communities Colonizing Drinking Water Distribution Pipes.
Lane, D.J., 1991. 16S/23S rRNA sequencing. In: Stackebrandt, E., Goodfellow, M. (Eds.), Nucleic Acid Techniques in Bacterial Systematics. John Wiley and Sons, New York, pp. 115–175.
Lehtola, M.J., Miettinen, I.T., Keinänen, M.M., Kekki, T.K., Laine, O., Hirvonen, A., Vartiainen, T., Martikainen, P.J., 2004. Microbiology, chemistry and biofilm development in a pilot drinking water distribution system with copper and plastic pipes. Water Res. 38, 3769–3779.
Ling, F., Hwang, C., LeChevallier, M.W., Andersen, G.L., Liu, W.-T., 2016. Core-satellite populations and seasonality of water meter biofilms in a metropolitan drinking water distribution system. ISME J. 10, 582–595.
Liu, G., Bakker, G., Li, S., Vreeburg, J., Verberk, J., Medema, G., Liu, W., Van Dijk, J., 2014a. Pyrosequencing reveals bacterial communities in unchlorinated drinking water distribution system: an integral study of bulk water, suspended solids, loose deposits, and pipe wall biofilm. Environ. Sci. Technol. 48, 5467–5476.
Liu, R., Zhu, J., Yu, Z., Joshi, D., Zhang, H., Lin, W., Yang, M., 2014b. Molecular analysis of long-term biofilm formation on PVC and cast iron surfaces in drinking water distribution system. J. Environ. Sci. 26, 865–874.
Mamane-Gravetz, H., Linden, K.G., 2005. Relationship between physiochemical properties, aggregation and u.v. inactivation of isolated indigenous spores in water. J. Appl. Microbiol. 98, 351–363.
Martiny, A.C., Jorgensen, T.M., Albrechtsen, H.J., Arvin, E., Molin, S., 2003. Long-term succession of structure and diversity of a biofilm formed in a model drinking water distribution system. Appl. Environ. Microbiol. 69, 6899–6907.
McCoy, S.T., VanBriesen, J.M., 2012. Temporal variability of bacterial diversity in a chlorinated drinking water distribution system. J. Environ. Eng. 138, 786–795.
Miller, A.G., Budd, K., 1975. The development of an increased rate of Cl− uptake in the ascomycete Neocosmospora vasinfecta. Can. J. Microbiol. 21, 1211–1216.
Muyzer, G., Dewaal, E.C., Uitterlinden, A.G., 1993. Profiling of complex microbial populations by denaturing gradient gel electrophoresis analysis of polymerase chain reaction amplified genes coding for the 16S rRNA. Appl. Environ. Microbiol. 59, 695–700.
Oliveira, H.M.B., Santos, C., Paterson, R.R.M., Gusmão, N.B., Lima, N., 2016. Fungi from a groundwater-fed drinking water supply system in Brazil. Int. J. Environ. Res. Publ. Health 13, 304.
Pereira, V.J., Fernandes, D., Carvalho, G., Benoliel, M.J., San Romão, M.V., Barreto Crespo, M.T., 2010. Assessment of the presence and dynamics of fungi in drinking water sources using cultural and molecular methods. Water Res. 44, 4850–4859.
Prest, E.I., Weissbrodt, D.G., Hammes, F., van Loosdrecht, M.C.M., Vrouwenvelder, J.S., 2016. Long-term bacterial dynamics in a full-scale drinking water distribution system. PLoS One 11 e0164445.
Rashid, M.I., Mujawar, L.H., Shahzad, T., Almeelbi, T., Ismail, I.M.I., Oves, M., 2016. Bacteria and fungi can contribute to nutrients bioavailability and aggregate formation in degraded soils. Microbiol. Res. 183, 26–41.
Revetta, R.P., Gomez-Alvarez, V., Gerke, T.L., Santo Domingo, J.W., Ashbolt, N.J., 2016. Changes in bacterial composition of biofilm in a metropolitan drinking water distribution system. J. Appl. Microbiol. 121, 294–305.
Revetta, R.P., Pemberton, A., Lamendella, R., Iker, B., Santo Domingo, J.W., 2010. Identification of bacterial populations in drinking water using 16S rRNA-based sequence analyses. Water Res. 44, 1353–1360.
Roeselers, G., Coolen, J., van der Wielen, P.W.J.J., Jaspers, M.C., Atsma, A., de Graaf, B., Schuren, F., 2015. Microbial biogeography of drinking water: patterns in phylogenetic diversity across space and time. Environ. Microbiol. 17, 2505–2514.
Schwering, M., Song, J., Louie, M., Turner, R.J., Ceri, H., 2013. Multi-species biofilms defined from drinking water microorganisms provide increased protection against chlorine disinfection. Biofouling 29, 917–928.
Simões, L.C., Chaves, A.F., Simões, M., Lima, N., 2016. The role of inter-kingdom interactions in chlorine resistance of biofilms formed by drinking water-isolated microorganisms. Biofilms 7, 165–165.
Simoes, L.C., Simoes, M., Vieira, M.J., 2010. Adhesion and biofilm formation on polystyrene by drinking water-isolated bacteria. Antonie Leeuwenhoek 98, 317–329.
Siqueira, V.M., Oliveira, H.M.B., Santos, C., Paterson, R.R.M., Gusmão, N.B., Lima, N., 2012. Biofilms from a Brazilian water distribution system include filamentous fungi. Can. J. Microbiol. 59, 183–188.
Sonigo, P., De Toni, A., Reilly, K., 2011. A Review of Fungi in Drinking Water and the Implications for Human Health. Report. Bio Intelligent Service, France.
van der Wielen, P.W., van der Kooij, D., 2010. Effect of water composition, distance and season on the adenosine triphosphate concentration in unchlorinated drinking water in The Netherlands. Water Res. 44, 4860–4867.
Vaz-Moreira, I., Nunes, O.C., Manaia, C.M., 2017. Ubiquitous and persistent Proteobacteria and other Gram-negative bacteria in drinking water. Sci. Total Environ. 586, 1141–1149.
Vilgalys, R., Hester, M., 1990. Rapid genetic identification and mapping of enzymatically amplified ribosomal DNA from several Cryptococcus species. J. Bacteriol. 172, 4238–4246.
Wang, H., Hu, C., Hu, X., Yang, M., Qu, J., 2012. Effects of disinfectant and biofilm on the corrosion of cast iron pipes in a reclaimed water distribution system. Water Res. 46, 1070–1078.
Wingender, J., Flemming, H.C., 2011. Biofilms in drinking water and their role as reservoir for pathogens. Int. J. Hyg Environ. Health 214, 417–423.
World Health Organization, 2006. Health Aspects of Plumbing.
Yooseph, S., Nealson, K.H., Rusch, D.B., McCrow, J.P., Dupont, C.L., Kim, M., Johnson, J., Montgomery, R., Ferriera, S., Beeson, K., Williamson, S.J., Tovchigrechko, A., Allen, A.E., Zeigler, L.A., Sutton, G., Eisenstadt, E., Rogers, Y.H., Friedman, R., Frazier, M., Venter, J.C., 2010. Genomic and functional adaptation in surface ocean planktonic prokaryotes. Nature 468, 60–66.
Zacheus, O.M., Martikainen, P.J., 1995. Occurrence of heterotrophic bacteria and fungi in cold and hot water distribution systems using water of different quality. Can. J. Microbiol. 41, 1088–1094.